Journal of Materials Chemistry A

PAPER

View Article Online
View Journal | View Issue

Cite this: J. Mater. Chem. A, 2014, 2, 1897

A novel "energy fiber" by coaxially integrating dye-sensitized solar cell and electrochemical capacitor†

Xuli Chen, Hao Sun, Zhibin Yang, Guozhen Guan, Zhitao Zhang, Longbin Qiu and Huisheng Peng*

Received 16th September 2013
Accepted 11th November 2013

DOI: 10.1039/c3ta13712k

www.rsc.org/MaterialsA

Dye-sensitized solar cell and electrochemical capacitor have been coaxially integrated into a novel "energy fiber" that can simultaneously realize photoelectric conversion and energy storage. A Ti wire substrate modified with perpendicularly aligned titania nanotubes on the surface and horizontally aligned multi-walled carbon nanotube sheet serve as two electrodes in the integrated "energy fiber" device. The "energy fiber" is flexible, and can be woven into various structures such as lightweight textiles to meet the portable facilities in the electronics.

Introduction

Portable devices represent a mainstream direction in the current and future electronics.[1–4] However, the conventional planar structure in energy devices cannot effectively meet the requirements such as being lightweight and deformable. To this end, some attempts have been recently made to develop wire-shaped solar cells and energy storage devices.[5–9] For the wire-shaped solar cell, both dye-sensitized and polymer solar cells have been explored. Polymer solar cells can be made without liquid components and with high stability, but they show low energy conversion efficiencies. In contrast, wire-shaped dye-sensitized solar cells can be fabricated with higher energy conversion efficiencies, though the use of liquid electrolytes has largely limited their performances such as low mechanical and thermal stabilities. It becomes critically important to make wire-shaped solar cells with both high efficiencies and stabilities. A general and effective solution may lie in the development of dye-sensitized solar cells without using liquid components, which has not been explored yet. For the wire-shaped energy storage device, electrochemical capacitors have been mainly investigated.[10–14] These wire-shaped energy conversion and storage devices were prepared by either twisting two fiber electrodes together or winding a membrane electrode on another fiber electrode. They typically exhibited diameters of tens to hundreds of micrometers with light weights. The wire-shaped devices are also flexible and can be easily woven into various textiles or other deformable structures according to the specific requirements.

State Key Laboratory of Molecular Engineering of Polymers, Department of Macromolecular Science, Laboratory of Advanced Materials, Fudan University, Shanghai 200438, China. E-mail: penghs@fudan.edu.cn

† Electronic supplementary information (ESI) available. See DOI: 10.1039/c3ta13712k

To promote their practical applications, it is critically important to integrate solar cells and electrochemical capacitors in a wire format.[15–19] Therefore, the resulting flexible structures such as electronic textiles can simultaneously realize the photoelectric conversion and energy storage for self-powered applications. A dye-sensitize solar cell and electrochemical capacitor were recently integrated by twisting two fiber electrodes together.[20] However, the twisted two fiber electrodes were found to be separated from each other under bending. In addition, the liquid electrolyte in the dye-sensitized solar cell was diffused into the electrochemical capacitor part. It is crucial, although it remains challenging, to improve the stability.[21–24]

Herein, we report a novel, coaxial, all-solid-state "energy fiber" by integrating dye-sensitized solar cell and electrochemical capacitor. A Ti wire substrate modified with perpendicularly aligned titania nanotubes on the surface and horizontally aligned carbon nanotube (CNT) sheets serve as two electrodes in the integrated "energy fiber" device. The maximal photoelectric conversion efficiency achieved 2.73%, while the energy storage efficiency reached 75.7% with specific capacitances up to 0.156 mF cm^{-1} or 3.32 mF cm^{-2} and power densities up to 0.013 mW cm^{-1} or 0.27 mW cm^{-2} at a current of 50 μA.

Experimental section

CNT sheets were drawn from CNT arrays that had been synthesized by chemical vapor deposition, and the preparations are detailed in the ESI.†[25,26] TiO_2 nanotubes were synthesized on commercially available Ti wires (diameter of 127 μm and purity of 99.9%) by electrochemical anodization. The anodization occurred at a voltage of 60 V for 1–10 h in a two-electrode electrochemical cell. A 0.3 wt% NH_4F/8 wt% H_2O–ethylene glycol mixture solution was used as the electrolyte. Ti wire and Pt sheet served as anode and cathode, respectively. The

modified Ti wires were washed by deionized water for three times to remove the residual electrolyte and then heated to and annealed at 500 °C in air for 1 h. The resulting TiO_2 nanotube-modified Ti wires were immersed in 40 mM $TiCl_4$ aqueous solution and treated at 70 °C for 30 min and then washed by deionized water for three times. Finally, they were annealed at 450 °C for another 30 min in air, followed by cooling down to room temperature naturally.

For the photoelectric conversion part, when the temperature dropped to 120 °C, the TiO_2 nanotube-modified Ti wire was immersed into 0.3 mM N719 solution in a mixture solvent of dehydrated acetonitrile/*tert*-butanol with a volume ratio of 1/1 for 16 h. A layer of CNT sheet (with a thickness of 20 nm) was then wrapped onto the dye-absorbed modified Ti wire that functioned as the working electrode. Thicker CNT sheets were prepared by repeating the winding process. The resulting fiber was further inserted into a transparent fluorinated ethylene propylene tube with a diameter of 500 μm (Shanghai Yi Chuan Shui Plastic Products Co.), followed by injection of the melted solid-state electrolyte, *i.e.*, a mixture of 1 g of ionic liquid crystal of 1-ethyl-3-methylimidazolium iodide (EMII), 0.35 g of ionic liquid of 1-propyl-3-methylimidazolium iodide (PMII) and 0.03 g of iodine.[27] During the measurement, the light was irradiated onto the solar cell in a perpendicular direction.

For the electrochemical storage part, the TiO_2 nanotube-modified Ti wire was coated with a gel electrolyte of PVA/H_3PO_4 with a mass ratio of 1/0.85. More details were provided in the ESI.† The CNT sheet was wrapped onto the following Ti wire. To make the capacitor more stable, a second layer of PVA/H_3PO_4 gel electrolyte was further coated on the outer surface.

The structures were characterized by scanning electron microscopy (SEM, Hitachi, FE-SEM S-4800 operated at 1 kV). The photoelectric conversion measurements were made by a Keithley 2400 Source Meter under illumination (100 mW cm^{-2}) of simulated AM 1.5 solar light provided by a solar simulator (Oriel-Sol3A 94023A equipped with a 450 W Xe lamp and an AM 1.5 filter). Galvanostatic charge–discharge characterizations were measured by an Arbin multi-channel electro-chemical testing system (Arbin, MSTAT-5 V/10 mA/16 Ch). Cyclic voltammetry and electrochemical impedance spectroscopy were performed on an electrochemical analyzer system (CHI 660D). The electrochemical impedance spectroscopy measurement had been made at a potential of 0.1 V and the frequency range from 100 MHz to 1 MHz.

Results and discussion

Fig. 1a schematically shows the structure and charging–discharging mechanism of the integrated "energy fiber". After absorbance of solar energy, the photoelectric conversion (PC) part generates electric energy that is stored in the electrochemical storage (ES) part when the switch is turned on to the red line. The stored electric energy can be used to power electronic devices by connecting them to the blue line and turning on the switch to the blue line. More details on the charging–discharging processes are provided in the ESI.† Fig. 1b and c represent cross-sectional schemes of the PC and ES parts,

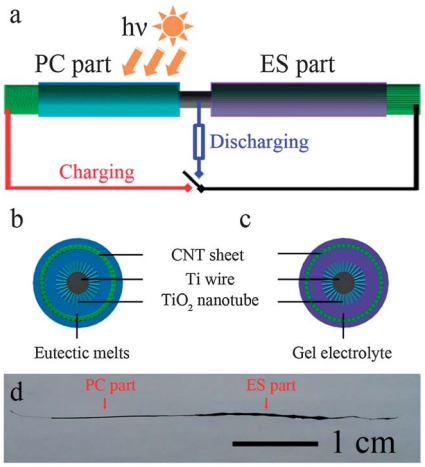

Fig. 1 (a) Schematic illustration of the structure of the coaxially integrated dye-sensitized solar cell and electrochemical capacitor into an "energy fiber". (b and c) Cross-sectional views of the PC and ES parts of the "energy fiber", respectively. (d) Photograph of an "energy fiber".

respectively. The center Ti wire is perpendicularly grown with aligned TiO_2 nanotube on the surface and serves as a negative electrode,[21] while a thin layer of CNT sheet has been wound to function as the positive electrode in both cases. Eutectic melts of ionic liquid crystal (EMII) and ionic liquid (PMII) with iodine had been used in the PC part, and a PVA/H_3PO_4 gel was used as the electrolyte in the ES part. Fig. 1d shows the photograph of a typical integrated "energy fiber".

The structure of the coaxially integrated "energy fiber" has been investigated by scanning electron microscopy (SEM). A Ti wire with a diameter of 127 μm was used as the substrate (Fig. 2a), and TiO_2 nanotubes should have been uniformly grown on the Ti wire as it remained uniform in diameter (Fig. 2b). A layer of aligned CNT sheet can be then wound on the TiO_2 nanotube-modified Ti wire (Fig. 2c and d). After anodization, the resulting wire showed an increased diameter to 150 μm (Fig. 2b). According to the cross-sectional image in Fig. 2e, the diameter of the Ti wire was decreased to 100 μm, so the thickness of the TiO_2 nanotube may be calculated to be appropriately 25 μm. TiO_2 nanotubes were perpendicularly grown on the Ti wire (Fig. 2f). The PC part would be completed after incorporation of the melted solid electrolyte. For the ES part, a layer of PVA/H_3PO_4 gel electrolyte was firstly coated onto the TiO_2 nanotube-modified Ti wire, followed by winding of the aligned CNT sheet and coating of a second layer of the same gel electrolyte. Therefore, five circles, *i.e.*, Ti wire, TiO_2 nanotube, gel electrolyte, aligned CNT sheet and gel electrolyte in the radial direction, are verified (Fig. 2e). The PVA/H_3PO_4 gel electrolyte had been efficiently infiltrated into the aligned TiO_2 nanotubes and CNTs with high surface areas (Fig. 2g and h), which provides high energy storage efficiencies. It should be also noted that the TiO_2 nanotubes and wound CNTs remained highly aligned after the incorporation of electrolytes (Fig. 2f and g), which is a key to the high performance of the "energy fiber" as the aligned nanotubes function as effective pathways for the charge transport.

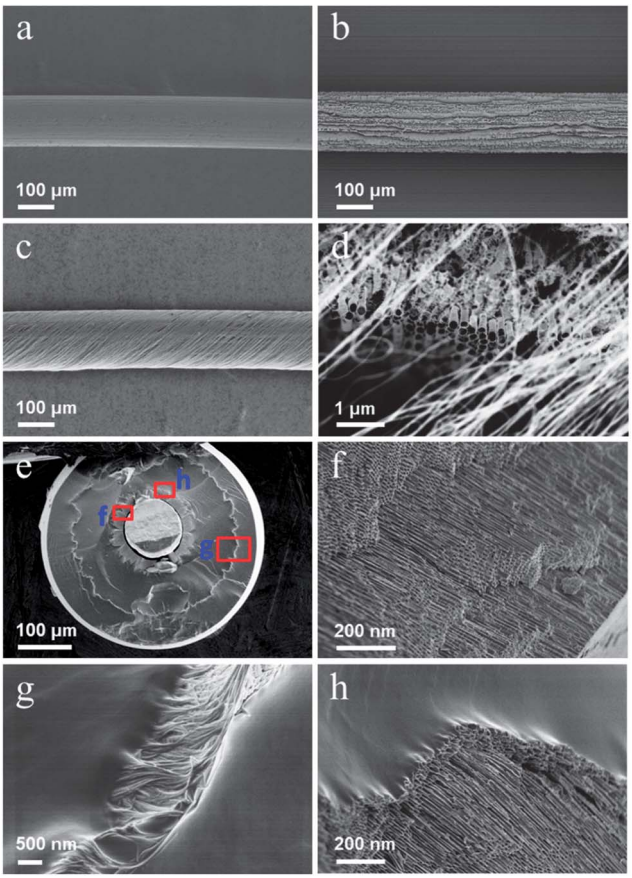

Fig. 2 SEM images. (a) Ti wire. (b) TiO_2 nanotubes grown on the Ti wire. (c and d) CNT sheet wrapped on the TiO_2 nanotubes for the PC part at low and high magnifications, respectively. (e) Cross-sectional image of the energy storage part. (f–h) Magnified images of the red rectangular areas at (e).

Fig. 3 represents a typical *J–V* curve of the PC part under the illumination condition of standard AM 1.5 (a power density of 100 mW cm^{-2}). Here the CNT sheet with a thickness of 20 nm and TiO_2 nanotubes with a length of 25 μm on the Ti wire served as counter and working electrodes, respectively. The open circle voltage (V_{oc}), short circle current density (J_{sc}) and fill factor (FF) were 0.635 V, 7.29 mA·cm^{-2} and 0.59, respectively. Therefore, the energy conversion efficiency can be calculated to be 2.73%.

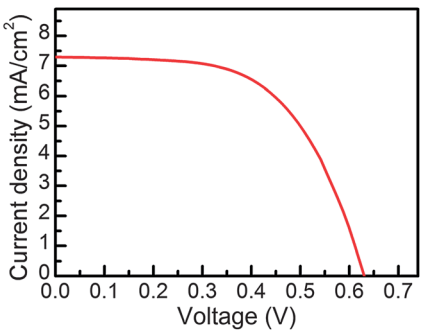

Fig. 3 *J–V* curve of the PC part under the illumination of AM 1.5.

Although the efficiency was relatively lower than the wire-shaped dye-sensitized solar cell based on the conventional liquid electrolyte, the use of the eutectic melts provides the PC part with both much higher thermal and mechanical stability.[20] For liquid electrolytes, the use of an acetonitrile solvent with a boiling point of 81.1 °C resulted in much decreased energy conversion efficiencies by 54.0% from room temperature to 70 °C, while for the PC part, a high performance had been well maintained even at temperatures up to 120 °C by tracing the *J–V* curve.[28] The energy conversion efficiencies were varied in less than 8.0% during heating. In addition, for the reported wire-shaped dye-sensitized solar cell based on a twisted structure, the two twisted fiber electrodes were separated during bending, which had decreased the energy conversion efficiency by 18.1% after bending for 100 cycles; for the PC part with a coaxial fiber structure, the energy conversion efficiencies were slightly decreased by 3.9% after bending for the same cycle number (Fig. S1†).

The electrochemical properties of the ES part had been carefully studied. Fig. 4a shows Galvanostatic charge–discharge curves at a current range from 1.00×10^{-7} to 1.00×10^{-5} A. All curves appeared in a symmetric, triangle shape that indicated an electric double-layer capacitor. To investigate the cyclic performance at different currents, cyclic charging–discharging characterizations were also made with the increasing current from 2.00×10^{-7} to 1.00×10^{-5} A (Fig. 4b). The Coulomb efficiencies had been increased from 94% to appropriately 100%, and the specific capacitances could be maintained by 80.8%. Fig. 4c further shows that the specific capacitances remain unchanged in 8000 cycles at a current of 1.00×10^{-5} A. Cyclic voltammograms were compared at increasing scan rates of 10, 20, 50, 100, 200, 500 and 1000 mV s^{-1} (Fig. 4d). They maintained a rectangular shape that also verified an electric double-layer capacitor in Fig. 4a. Here the maintained rectangular shape also demonstrates that the ES part had a low internal resistance and high performance in a rapid charging–discharging characterization.

The ES part was also investigated by electrochemical impedance spectroscopy (Fig. 4e). The 90° inclination in the Nyquist plot demonstrated a nearly perfect capacitor performance of the device. The difference of horizontal intercepts between black square and red triangular plots also indicates that the internal resistances are decreased with the increasing CNT thickness. Fig. 4f shows that, with the increase in CNT thickness, the length specific capacitances are increased and reach a plateau value of 0.156 mF cm^{-1} (*i.e.*, 3.32 mF cm^{-2}, Fig. S2†) at 10 μm. This phenomenon indicates that the electrolyte can be mainly infiltrated into the CNT sheet material with a thickness of 10 μm. Here a thickness of 500 nm had been mainly studied in the following discussion if not specified, aiming at the future development for miniature and lightweight devices.

Fig. 5a shows a typical photocharging and galvanostatic discharging curve at a discharging current of 1 μA. The ES part had been quickly charged to a plateau voltage of 0.63 V, appropriately equal to the V_{oc} of the PC part. It was then discharged at the current of 1 μA to 0.005 V. The energy storage

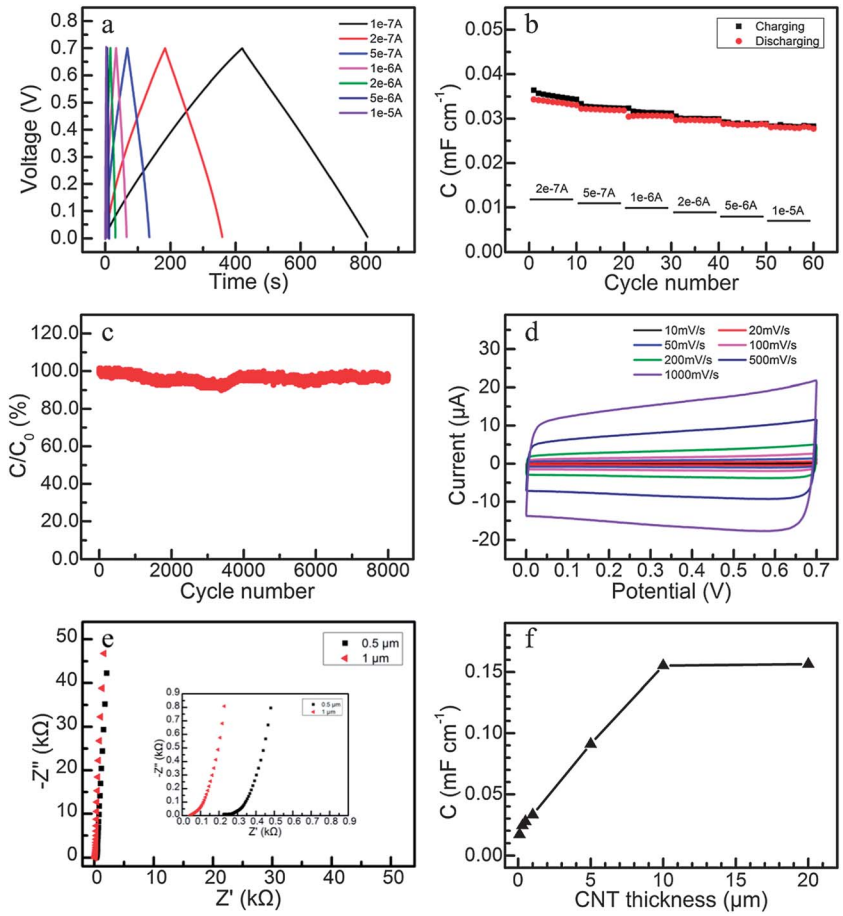

Fig. 4 Electrochemical characterizations of the ES part. (a) Galvanostatic charge–discharge curves under currents ranging from 1.00×10^{-7} to 1.00×10^{-5} A. (b) Cyclic performance at the increasing electric current. (c) Long life cyclic performance at a current of 1.00×10^{-5} A. C_0 and C correspond to the specific capacitances of the first and following cycles, respectively. (d) CV curves with increasing scan rates. (e) Nyquist plot of the "energy fiber" with different CNT thicknesses. (f) Dependence of specific capacitance on the CNT thickness. The cyclic galvanostatic charge–discharge measurements were made at a current of 1.00×10^{-6} A.

efficiency ($\eta_{storage}$) and entire photovoltaic conversion and energy storage efficiency (η) were calculated from the following equations

$$\eta_{storage} = \frac{\int UdQ}{E_{in}\eta_{conver}} = \frac{0.5\ It_{discharge}(U_2 - U_1)}{P_{in}t_{charge}Dl\eta_{conver}} \quad (1)$$

$$\eta = \frac{\int UdQ}{E_{in}} = \frac{0.5\ It_{discharge}(U_2 - U_1)}{P_{in}t_{charge}Dl} \quad (2)$$

Here Q is the electric charge of galvanostatic discharging process; E_{in} and η_{conver} are the incident solar energy and energy conversion efficiency of PC part during the photocharging process, respectively; I is the galvanostatic discharging current of 1 μA; $t_{discharge}$ is the discharging time; U_1 and U_2 are the lowest and highest voltages, respectively; P_{in} is the illuminated light-energy density of 1000 W m^{-2}; t_{charge} is the photocharging time; D and l are the diameter and length of the PC part, respectively. The voltages and energy storage efficiencies were varied during the photocharging and galvanostatic discharging process (Fig. 5b). The voltage was rapidly increased and reached the plateau in a second at the beginning of the photocharging process. The energy storage efficiency was firstly increased to a maximum of appropriately 60% in a second and then decreased to the plateau of 5% in ~9 seconds. The $\eta_{conversion}$ values were largely dependent on the length of TiO_2 nanotubes, and an optimal length of 25 μm had been discovered for these systems (Fig. S3†).[29,30] Therefore, TiO_2 nanotube with a length of 25 μm was generally used in this work. On the other hand, the η values were decreased with the increasing CNT sheet (Fig. 5c), and a maximum of 1.2% had been achieved at ~20 nm which had been mainly used for the following PC part (note that here the CNT thickness was 500 nm in the ES part). This phenomenon can be explained by the fact that the optical transmittances were decreased with the increasing thickness of CNT sheet, which reduced the current density of the PC part (Fig. S4†). In addition, the critical photo-charging time to the voltage plateau was also increased with the increase of the CNT sheet due to the reduced photocharging current, so the ES part can be more rapidly charged for thinner CNT sheets. The energy storage efficiencies were increased with the increasing CNT sheet

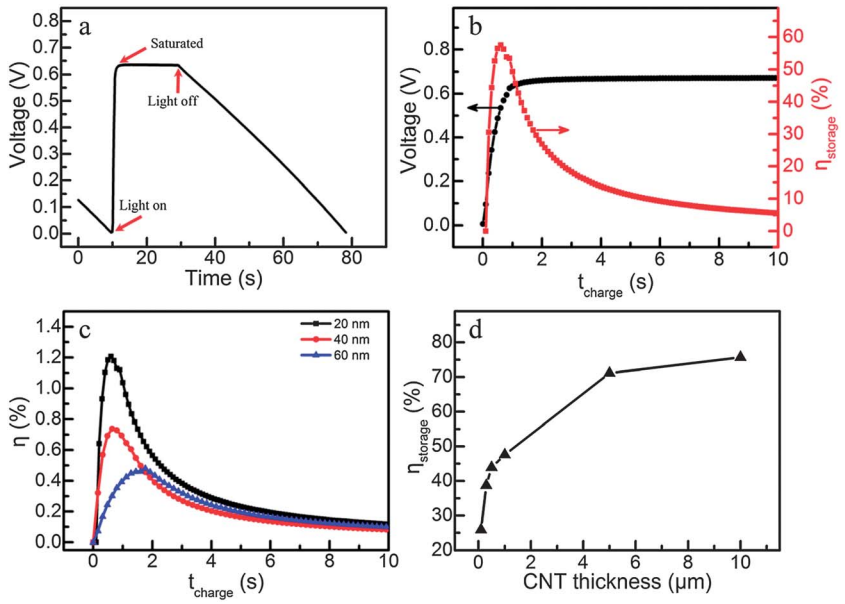

Fig. 5 (a) A typical photocharging and Galvanostatic discharging curve. (b) Dependence of voltage and storage efficiency on the photocharging time during the photocharging and Galvanostatic discharging process. (c) Dependence of entire photoelectric conversion and storage efficiency on CNT thickness in the PC part on the photocharging time. (d) Dependence of energy storage efficiency on CNT thickness in the ES part.

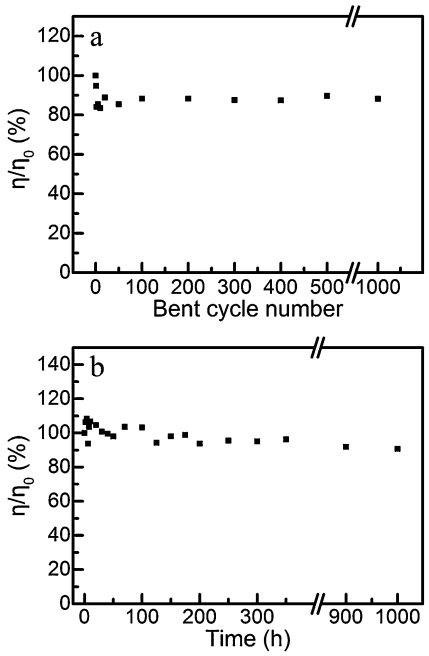

Fig. 6 (a) Dependence of entire photoelectric conversion and storage efficiency on the bent cycle number. η_0 and η correspond to the entire photoelectric conversion and storage efficiencies before and after bending, respectively. (b) Dependence of entire photoelectric conversion and storage efficiency on the time. η_0 and η correspond to the entire photoelectric conversion and storage efficiencies of the as-fabricated device and the one at the following measured time, respectively.

thickness and reached a plateau of 75% at 10 μm (Fig. 5d), which agrees with Fig. 4f. At the same time, the specific capacitance and energy storage efficiency were increased with the increasing TiO_2 nanotube length to 16 μm and then possibly reached a plateau (Fig. S5†). This phenomenon may be explained by the fact that the TiO_2 nanotubes cannot be fully filled with gel electrolyte beyond the critical length of 16 μm.

This integrated "energy fiber" was flexible and could be deformed without obvious fatigues in both structural integrity and electronic properties. Fig. 6a shows the dependence of the entire photoelectric conversion and energy storage efficiency on bent cycle number. The entire efficiency had been maintained by 88.2% even after bending for 1000 cycles (Fig. S6†). In addition, the entire efficiency of the "energy fiber" could be maintained by 90.6% after 1000 hours (Fig. 6b).

Conclusion

In summary, we have developed a novel coaxial, all-solid-state, fiber-shaped "energy fiber" that can simultaneously realize energy conversion and storage by integrating dye-sensitized solar cell and electrochemical capacitor. The photoelectric conversion and energy storage efficiencies currently reach 2.73% and 75.7%, respectively. More efforts are underway to further improve them by optimizing the structure. The "energy fiber" is flexible and stable, and shows promising applications for various portable electronic devices that require lightweight and weaveable materials.

Acknowledgements

This work was supported by NSFC (91027025, 21225417), MOST (2011CB932503, 2011DFA51330), STCSM (11520701400, 12nm0503200), Fok Ying Tong Education Foundation, Innovative Student Program at Fudan University (EZH2203302/002),

the Program for Professor of Special Appointment at Shanghai Institutions of Higher Learning, and the Program for Outstanding Young Scholars from Organization Department of the CPC Central Committee.

References

1 N. Li, S. Oida, G. S. Tulevski, S.-J. Han, J. B. Hannon, D. K. Sadana and T.-C. Chen, *Nat. Commun.*, 2013, **4**, 2294.
2 H. K. Yu, S. Kim, B. Koo, G. H. Jung, B. Lee, J. Ham and J. L. Lee, *Nanoscale*, 2012, **4**, 6831.
3 C. Yang, W. Lin, Z. Li, R. Zhang, H. Wen, B. Gao, G. Chen, P. Gao, M. M. F. Yuen and C. P. Wong, *Adv. Funct. Mater.*, 2011, **21**, 4582.
4 C. Yang, H. Gu, W. Lin, M. M. Yuen, C. P. Wong, M. Xiong and B. Gao, *Adv. Mater.*, 2011, **23**, 3052.
5 T. Chen, L. Qiu, Z. Cai, F. Gong, Z. Yang, Z. Wang and H. Peng, *Nano Lett.*, 2012, **12**, 2568.
6 S. Zhang, C. Ji, Z. Bian, R. Liu, X. Xia, D. Yun, L. Zhang, C. Huang and A. Cao, *Nano Lett.*, 2011, **11**, 3383.
7 T. Chen, S. Wang, Z. Yang, Q. Feng, X. Sun, L. Li, Z.-S. Wang and H. Peng, *Angew. Chem., Int. Ed.*, 2011, **50**, 1815.
8 S. Berson, R. De Bettignies, S. Bailly and S. Guillerez, *Adv. Funct. Mater.*, 2007, **17**, 1377.
9 D. Liu, M. Zhao, Y. Li, Z. Bian, L. Zhang, Y. Shang, X. Xia, S. Zhang, D. Yun, Z. Liu, A. Cao and C. Huang, *ACS Nano*, 2012, **6**, 11027.
10 Z. Cai, L. Li, J. Ren, L. Qiu, H. Lin and H. Peng, *J. Mater. Chem. A*, 2013, **1**, 258.
11 Z. Gui, H. Zhu, E. Gillette, X. Han, G. W. Rubloff, L. Hu and S. B. Lee, *ACS Nano*, 2013, **7**, 6037.
12 J. Ren, L. Li, C. Chen, X. Chen, Z. Cai, L. Qiu, Y. Wang, X. Zhu and H. Peng, *Adv. Mater.*, 2013, **25**, 1155.
13 J. Bae, M. K. Song, Y. J. Park, J. M. Kim, M. Liu and Z. L. Wang, *Angew. Chem., Int. Ed.*, 2011, **50**, 1683.
14 V. T. Le, H. Kim, A. Ghosh, J. Kim, J. Chang, Q. A. Vu, D. T. Pham, J.-H. Lee, S.-W. Kim and Y. H. Lee, *ACS Nano*, 2013, **7**, 5940.
15 N. S. Lewis, *Science*, 2007, **315**, 798.
16 Z. Yang, L. Li, Y. Luo, R. He, L. Qiu, H. Lin and H. Peng, *J. Mater. Chem. A*, 2013, **1**, 954.
17 W. Guo, X. Xue, S. Wang, C. Lin and Z. L. Wang, *Nano Lett.*, 2012, **12**, 2520.
18 T. N. Murakami, N. Kawashima and T. Miyasaka, *Chem. Commun.*, 2005, 3346.
19 G. Wee, T. Salim, Y. M. Lam, S. G. Mhaisalkar and M. Srinivasan, *Energy Environ. Sci.*, 2011, **4**, 413.
20 T. Chen, L. Qiu, Z. Yang, Z. Cai, J. Ren, H. Li, H. Lin, X. Sun and H. Peng, *Angew. Chem., Int. Ed.*, 2012, **51**, 11977.
21 T. Chen, L. Qiu, H. G. Kia, Z. Yang and H. Peng, *Adv. Mater.*, 2012, **24**, 4623.
22 H. C. Weerasinghe, F. Huang and Y.-B. Cheng, *Nano Energy*, 2013, **2**, 174.
23 T. Chen, L. Qiu, Z. Yang and H. Peng, *Chem. Soc. Rev.*, 2013, **42**, 5031.
24 P. Wang, S. M. Zakeeruddin, P. Comte, I. Exnar and M. Grätzel, *J. Am. Chem. Soc.*, 2003, **125**, 1166.
25 Z. Yang, T. Chen, R. He, G. Guan, H. Li, L. Qiu and H. Peng, *Adv. Mater.*, 2011, **23**, 5436.
26 H. Peng, X. Sun, F. Cai, X. Chen, Y. Zhu, G. Liao, D. Chen, Q. Li, Y. Lu, Y. Zhu and Q. Jia, *Nat. Nanotechnol.*, 2009, **4**, 738.
27 E. I. Izgorodina, R. Maganti, V. Armel, P. M. Dean, J. M. Pringle, K. R. Seddon and D. R. MacFarlane, *J. Phys. Chem. B*, 2011, **115**, 14688.
28 H. Sun, H. Li, X. You, Z. Yang, J. Deng, L. Qiu and H. Peng, *J. Mater. Chem. A*, 2014, **2**, 345.
29 L. Chen, Y. Zhou, H. Dai, Z. Li, T. Yu, J. Liu and Z. Zou, *J. Mater. Chem. A*, 2013, **1**, 11790.
30 H. Sun, X. You, Z. Yang, J. Deng and H. Peng, *J. Mater. Chem. A*, 2013, **1**, 12422.

